JOURNAL OF SOLID STATE CHEMISTRY 120, 101–104 (1995)

Structure of $Zr_2(WO_4)(PO_4)_2$ from Powder X-Ray Data: Cation Ordering with No Superstructure

J. S. O. Evans, T. A. Mary, and A. W. Sleight

Department of Chemistry and Center for Advanced Materials Research, Oregon State University, Corvallis, Oregon

Received April 21, 1995; in revised form July 13, 1995; accepted July 19, 1995

The ab initio structure determination of $Zr_2(WO_4)(PO_4)_2$ from room temperature powder X-ray diffraction data is reported. This compound crystallizes in the orthorhombic space group *Pnca* with $a = 9.35451(9)$, $b = 12.31831(9)$, and $c = 9.16711(8)$ Å. The structure is based on ZrO_6 octahedra sharing corners with WO_4 and PO_4 tetrahedra. Although $Zr_2(WO_4)(PO_4)_2$ is isostructural with $Fe_2(MoO_4)_3$ and its WO_4 and PO_4 tetrahedra are well ordered, no superstructure or change in space group is required to account for this ordering.

INTRODUCTION

Several phases in the Zr/V/P/O and Zr/W/O systems are of interest for their low, and in some cases negative, coefficients of thermal expansion (1, 2). During recent investigations on the system Zr/W/P/O, we have prepared the phase first reported by Martinek *et al.* as $2ZrO_2 \cdot WO_3 \cdot P_2O_5$, whose unit cell constants have recently been reported by Tsvigunov *et al.* (3, 4). The structure of this phase has been solved from laboratory powder X-ray data using Patterson and direct methods followed by refinement using Rietveld methods. The structure contains corner sharing ZrO_6 octahedra and WO_4 and PO_4 tetrahedra which give rise to a framework lattice and vacant channels through the structure. The polyhedral arrangement is similar to that of garnet, $Ca_3Al_2(SiO_4)_3$, such that $Zr_2(WO_4)(PO_4)_2$ may be related to an A site vacant garnet. The title compound is, to our knowledge, the first structurally characterized example of the coexistence of WO_4 and PO_4 tetrahedra in one compound.

SYNTHESIS

Stoichiometric ratios of reagent grade ZrO_2, ZrP_2O_7 (Teledyne Wah Chang, USA), and WO_3 (99.9%, Cerac, USA) were mixed thoroughly, heated in a platinum crucible at 1200°C for 6 hr and then air cooled to room temperature. The sample was then ground and heated at 1250°C for a further 5 hr. A more crystalline sample, totally free of any minor impurities, was prepared for structural analysis by heating a stoichiometric ratio of the starting materials at 1250°C in a sealed silica ampoule followed by a slow cool to room temperature. The Zr : W : P ratio of the material was confirmed by electron microprobe analysis.

STRUCTURAL INVESTIGATION

Powder X-ray diffraction patterns were recorded at room temperature on a Siemens D5000 diffractometer equipped with computer controlled antiscatter slits, vertical Soller slits, and a Kevex detector; details of the data collection are given in Table 1. Accurate peak positions were obtained for 30 reflections using the Split–Pearson function within the Siemens DIFFRAC/AT software suite (5). Autoindexing (6) gave an orthorhombic cell [$a = 9.35451(9)$, $b = 12.31831(9)$, $c = 9.16711(8)$ Å] with a figure of merit, M_{20}, of 75.9; cell constants are similar to those previously reported (4). Careful examination of systematic absences, involving deconvolution of regions of peak overlap, suggested space group *Pnca* (number 60). Since successful refinement was achieved in this space group, no other alternatives were considered.

Integrated intensities were extracted for the first 150 reflections using the Lebail method within the GSAS software suite, and structure factors of $K\alpha_1$ and $K\alpha_2$ peaks were averaged (7). Structure solution was attempted by both direct methods using Sirpow92 and Patterson methods using SHELXS (8, 9). Both procedures suggested the same possible W site; direct methods also suggested a potential Zr site. Successive cycles of least-squares refinement and difference Fourier synthesis were performed using SHELXL-92 (10), but this revealed only two possible oxygen sites around the zirconium atom. No other reasonable atomic coordinates could be obtained. It was found, however, that introduction of a regular ZrO_6 octahedron (d Zr–O = 2.05 Å) based on the observed zirconium and oxygen positions gave rise to a distorted tetrahedral coordination of tungsten (W-O bonds of 1.77 and 1.84 Å). A potential (highly distorted) tetrahedral P site was then identified (P-O bonds ranging from 1.39 to 1.94 Å), and this structure was refined using distance least-squares (DLS)

0022-4596/95 $12.00

TABLE 1
Details of Data Collection and Refinement

a (Å)	9.35451(9)
b (Å)	12.31831(9)
c (Å)	9.16711(8)
Zero point (°)	−0.0166(2)
Spacegroup (Number)	*Pnca* (60)
Preferred orientation, R_o	0.849(2)
Suorrti absorption parameter	0.344
Data range (°2θ)	14.5–120
Step size (°2θ)	0.02
Time per step (sec)	8.0
Number of data points	5249
Number of reflections	1567
Number of variables	48
wR_p (%)	9.55
R_p (%)	7.12
R_F (%)	3.15
χ^2	5.26

Note. Symbols have their usual meaning, or are as defined in the GSAS manual. Estimated standard deviations given in parentheses are those reported by GSAS. Standard deviations on the unit cell dimensions are consequently an underestimate of the true errors.

methods (11). Five cycles of DLS refinement successfully regularized the coordination polyhedra.

The DLS solution was then used as a starting model for Rietveld refinement using the GSAS package. It became apparent early in the refinement that the sample exhibited extreme (010) preferred orientation. Tests showed that this could be reduced by packing the sample extremely loosely on the X-ray slide. For final cycles of refinement, data were re-collected using this technique. Due to this method of sample packing, the data showed effects due to the non-smooth nature of the powder surface. This causes a systematic reduction in the intensity of low angle peaks which results in slightly negative thermal parameters for all atoms. Data were consequently corrected for the effects of nonuniform porosity using the method of Suortti (12). Isotropic thermal parameters were fixed at values typical for this class of materials, and a porosity correction was applied. Temperature factors were subsequently allowed to refine freely. Using this protocol, an excellent fit to the observed data was obtained.

During final cycles of refinement, fractional atomic coordinates and temperature factors (34 variables), scale factor zero point, unit cell parameters, eight background terms, and a preferred orientation (March–Dollase) term were allowed to refine freely, giving final profile agreement factors of wR_p = 9.55%, R_p = 7.12%, and R_F = 3.15%. Observed and calculated profiles are shown in Figure 1. Full details of the refinement are given in Table 1, final atomic coordinates in Table 2, and selected bond distances and angles in Table 3.

Rietveld refinement was also performed on the less crystalline phase formed by a rapid cooling of the sample to room temperature. This sample refined successfully using the same structural model with no need for a preferred orientation correction [a = 9.3413(2); b = 12.3508(3); c = 9.1581(3); wR_p = 8.79%, R_p = 6.72%, R_F = 3.45%]. For reasons discussed below structural parameters based on the first refinement are reported.

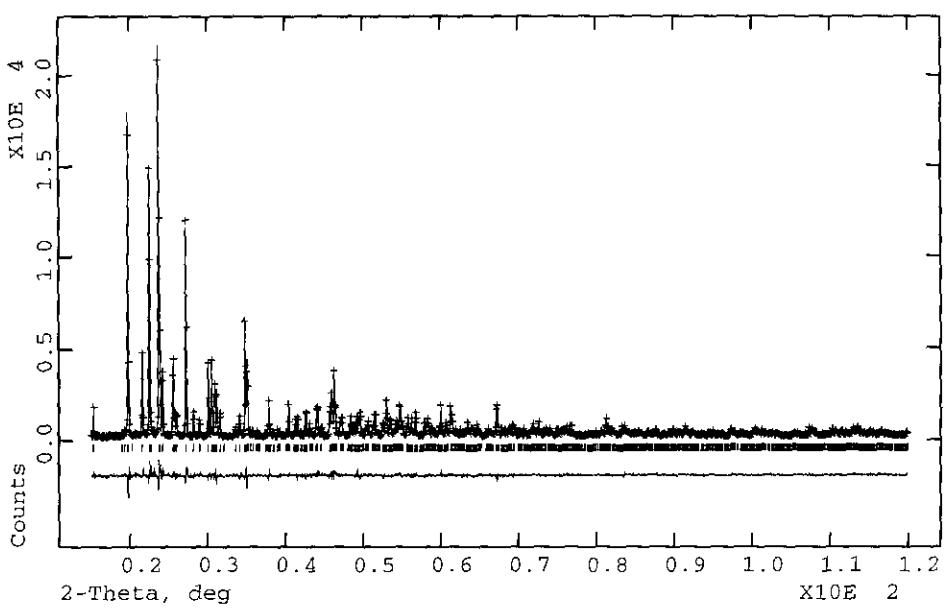

FIG. 1. Observed (+), calculated (—), and difference (lower trace) powder diffraction patterns of $Zr_2(WO_4)(PO_4)_2$.

TABLE 2
Fractional Atomic Coordinates

	x	y	z	U_{iso} (Å^2)
Zr1	0.04886(20)	0.36857(14)	0.22597(22)	0.0150(5)
W1	0.25	0.0	0.03975(17)	0.0168(4)
P1	0.6046(6)	0.8554(5)	0.3839(7)	0.014(2)
O1	0.8658(15)	0.4252(9)	0.3532(16)	0.036(5)
O2	0.9273(12)	0.3498(8)	0.0430(14)	0.011(3)
O3	0.0818(11)	0.5274(9)	0.1703(12)	0.016(4)
O4	−0.0030(14)	0.2174(8)	0.3005(14)	0.015(3)
O5	0.1560(13)	0.4024(9)	0.4284(13)	0.020(4)
O6	0.2461(18)	0.3282(7)	0.1420(12)	0.018(3)

Note. Estimated standard deviations in parentheses.

DISCUSSION OF THE STRUCTURE

Figure 2 shows views of the structure projected down the [001] and [100] axes. The structure consists of a corner sharing arrangement of ZrO_6 octahedra and WO_4/PO_4 tetrahedra. Each ZrO_6 octahedron shares corners with two WO_4 tetrahedra and four PO_4 tetrahedra; each tetrahedron shares corners with four different ZrO_6 octahedra. As expected from the difference in ionic radii, the coordination of the two tetrahedral sites differs significantly (average oxygen bond distances being 1.500 Å for the P site and 1.767 Å for the W site). This confirms that the tetrahedral cations are well ordered in the structure (vide infra). Table 3 shows that bond distances and angles fall within the expected ranges, with tetrahedral and octahedral angles close to the ideal. It can also be seen that zirconium oxygen bonds of the zirconium–oxygen–tungsten bridges are significantly longer (average 2.175 Å) than those of zirconium–oxygen–phosphorus bridges (average 2.046 Å).

The two methods of sample preparation (referred to hereafter as slow-cooled and fast-cooled) result in phases with slightly different cell parameters [the maximum difference being in the b-axis of 12.31831 (slow-cool) vs 12.3508 Å (fast-cool)]. Rietveld refinement suggests that this difference can be related to the degree of ordering of the tetrahedral cations. For the slow-cooled sample, no significant improvement in the quality of the X-ray fit could be obtained by introducing either partial occupancy or cation site disorder. In the case of the fast cooled sample, however, a small but significant improvement in the fit could be obtained by introducing partial disorder (up to 4% P on the W site) of the tetrahedral cations. For this reason structural parameters are reported based on refinement of the more crystalline phase, though it should be noted that the degree of preferred orientation may result in slight inaccuracies in atomic positions.

The structure of $Zr_2(WO_4)(PO_4)_2$ is closely related to the $A_2(MO_4)_3$ structures (M = Mo, A = Al, Sc, Cr, Fe, Y, In, Ho, Er, Tm, Yb, Lu; M = W, A = Al, Sc, Fe, In, Y, Gd, Tb, Dy, Ho, Yb, Tm, Yb, Lu) and also to $Fe_2(SO_4)_3$, which are either orthorhombic, *Pnca*, or monoclinic, $P2_1/a$ (13–18). Many of these systems exhibit a ferroelastic orthorhombic to monoclinic transition with decreasing temperature (15). The $A_2(MO_4)_3$ orthorhombic structure contains two crystallographically distinct tetrahedral groups which are chemically essentially equivalent. In $Zr_2(WO_4)(PO_4)_2$, one of these tetrahedral sites is occupied exclusively by tungsten and the other exclusively by phosphorus. Because this ordering of P and W produces no new crystallographic sites, the space group does not change and there is no superstructure.

The framework of these structures can be considered as related to that of garnet, $Ca_3Al_2(SiO_4)_3$ (19, 20). In garnet itself the framework of corner sharing octahedra and tetrahedra creates 8-coordinate sites which are occupied by calcium ions. The framework is, however, able to accommodate changes in A site occupancy or oxidation state, with charge balance being maintained by substitution on the tetrahedral or octahedral site. Thus, the structural relationship between the garnets and the $A_2(MO_4)_3$ compounds is perhaps best exemplified by the series of compounds $Y_3Fe_2(FeO_4)_3$, $Ca_3Al_2(SiO_4)_3$, $Na_3Al_2(PO_4)_3$, and $\square_3Fe_2(MoO_4)_3$ (20). This series shows how a stepwise reduction in the A site oxidation state from Y^{3+} down to the hypothetical $\square^{0+}$ (where $\square$ represents a vacancy site) is

TABLE 3
Selected Bond Distances (Å) and Angles (°)

	O1	O2	O3	O4	O5	O6
Zr1	2.186(13)	2.039(12)	2.045(12)	2.042(10)	2.149(13)	2.060(16)
W1	1.728(13)	× 2			1.806(12)	× 2
P1		1.491(12)	1.541(12)	1.514(12)		1.456(16)
O–W–O	110.8(9)	111.8(6)	105.7(5)			
O–P–O	109.3(7)	109.9(8)	109.9(7)	107.8(7)	107.2(7)	112.5(8)
W–O–Zr	164.6(7)					
Zr–O–P	155.7(8)	175.6(7)				

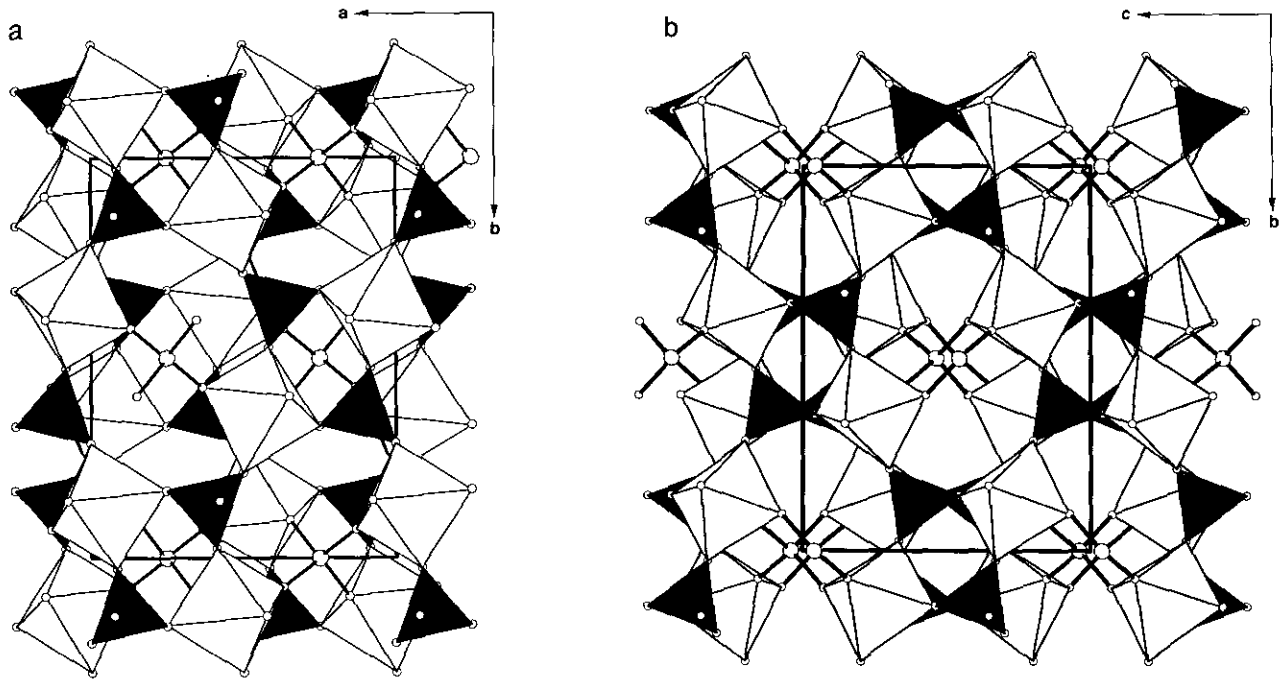

FIG. 2. The structure of $Zr_2(WO_4)(PO_4)_2$ viewed down (a) the [001] and (b) the [100] axes. ZrO_6 octahedra shown in white, PO_4 tetrahedra in grey, and tungsten atoms displayed as large open circles.

compensated by a corresponding increase in the oxidation state of the tetrahedral cation.

The A site vacancies lead to vacant channels running through the structure, suggesting the possibility of intercalating ionic species. A number of garnet related phases are of interest as potential fast ion conductors. Lithium insertion into both $Fe_2(MoO_4)_3$ and $Fe_2(WO_4)_3$ has been reported (21, 22). The possibility of lithium insertion into $Zr_2(WO_4)(PO_4)_2$ and related phases is being investigated.

Dilatometer and variable temperature X-ray diffraction studies have shown that $Zr_2(WO_4)(PO_4)_2$ displays unusual negative thermal expansion over a broad temperature range. A detailed study of the thermal properties of this and other structurally related phases will be reported elsewhere (23).

ACKNOWLEDGMENT

This work was supported by NSF Grant DMR-9308530.

REFERENCES

1. V. Korthuis, N. Khosrovani, A. W. Sleight, N. Roberts, R. Dupree, and W. W. Warren, *Chem. Mater.* **7,** 412 (1995).
2. T. A. Mary, J. S. O. Evans, and A. W. Sleight, in preparation, (1995).
3. C. A. Martinek and F. A. Hummel, *J. Am. Ceram. Soc.* **53,** 159 (1970).
4. A. N. Tsvigunov and V. P. Sirotinkin, *Russ. J. Inorg. Chem.* **35,** 1740 (1990).
5. A. Brown and J. W. Edmonds, *Adv. X-Ray Anal.* **23,** 361 (1980).
6. J. W. Visser, *J. Appl. Crystallogr.* **2,** 89 (1969).
7. A. C. Larson and R. B. Von Dreele, *LANSCE,* Los Alamos National Lab., 1994.
8. G. M. Sheldrick, *Acta Crystallogr. Sect. A* **46,** 467 (1990).
9. A. Altomare, G. Cascarano, C. Giacovazzo, A. Guagliardi, M. C. Burla, G. Polidori, and M. Camalli, *J. Appl. Crystallogr.* **27,** 435 (1994).
10. G. M. Sheldrick, University of Göttingen, 1992.
11. C. Baerlocher, A. Hepp, and W. M. Meier, Institute of Crystallography and Petrology, Eidgenössische Technische Hochschule, Switzerland, 1977.
12. P. Suortti, *J. Appl. Crystallogr.* **5,** 325 (1972).
13. S. C. Abrahams and J. L. Bernstein, *J. Chem. Phys.* **45,** 2745 (1966).
14. A. W. Briedl, *Acta. Crystallogr.* **19,** 1059 (1965).
15. A. W. Sleight and L. H. Brixner, *J. Solid State Chem.* **7,** 172 (1973).
16. G. J. Long, G. Longworth, P. D. Battle, A. K. Cheetham, R. V. Thundathil, and D. Beveridge, *Inorg. Chem.* **18,** 624 (1979).
17. P. D. Battle, A. K. Cheetham, G. J. Long, and G. Longworth, *Inorg. Chem.* **21,** 4223 (1982).
18. W. T. A. Harrison, U. Chowdhry, C. J. Machiels, A. W. Sleight, and A. K. Cheetham, *J. Solid State Chem.* **60,** 101 (1985).
19. Y. Piffard, A. Verbaere, and M. Kinoshita, *J. Solid State Chem.* **71,** 121 (1987).
20. L. M. Plysova, S. V. Borisov, and N. V. Belov, *Sov. Phys. Crystallogr. (Engl. Transl.)* **12,** 25 (1967).
21. W. M. Reiff, J. H. Zhang, and C. C. Torardi, *J. Solid State Chem.* **62,** 231 (1986).
22. A. Manthiram and J. B. Goodenough, *J. Solid State Chem.* **71,** 349 (1987).
23. T. A. Mary, J. S. O. Evans, and A. W. Sleight, unpublished results.